

## Multifractality of random walks in the theory of vehicular traffic

G. M. Buendía,<sup>1,2</sup> G. M. Viswanathan,<sup>1,3</sup> and V. M. Kenkre<sup>1</sup>

<sup>1</sup>*Consortium of the Americas for Interdisciplinary Science, University of New Mexico,  
800 Yale Boulevard NE, Albuquerque, New Mexico 87131, USA*

<sup>2</sup>*Physics Department, Universidad Simón Bolívar, Caracas 1080, Venezuela*

<sup>3</sup>*Instituto de Física, Universidade Federal de Alagoas, Maceió-AL, 57072-970, Brazil*

(Received 15 September 2008; published 25 November 2008)

We investigate the origin of the experimentally observed multifractal scaling of vehicular traffic flows by studying a hydrodynamic model of traffic. We first extend and apply the formalism of generalized Hurst exponents  $H(q)$  to the case of random walkers that not only diffuse but rather also undergo nonlinear convection due to interactions with other walkers. We recover analytically, as expected, that  $H(q)$  equals 1/2 for a single random walker starting at the origin whose probability density function satisfies Burger's equation. Despite this result for a single walker, we find that for a collection of nonlinearly convecting diffusive particles, transient effects can give rise to multiscaling at given time scales for many initial conditions. In the Lighthill-Whitham-Richards hydrodynamic model of traffic, this multiscaling effect becomes more prominent for smaller diffusion constants and larger speed limits. We discuss the relevance of these findings for the realistic scenario of traffic that flows from small roads to large highways and vice versa, where transient effects can be expected to play a significant role.

DOI: [10.1103/PhysRevE.78.056110](https://doi.org/10.1103/PhysRevE.78.056110)

PACS number(s): 89.40.-a, 47.53.+n, 45.70.Vn

### I. INTRODUCTION

Numerous studies designed to understand traffic problems [1–9] have led to significant advances in the quantitative description of self-propelled particles [10]. As is well known, the kinematics of particles can be approached on the one hand from the perspective of Langevin equations for the trajectories and on the other hand in terms of hydrodynamic equations for the density of particles. Generalized Hurst exponents and local Hölder exponents quantify the scaling properties of random walks [11–17]. Empirical studies of traffic flow [6–9] have shown multifractal rather than monofractal scaling, i.e., a single scaling exponent does not suffice for quantifying the scaling. The physical origin of this multifractal scaling is interesting to explore. Here we investigate multifractality and multiscaling from the perspective of the Lighthill-Whitham-Richards hydrodynamic model of traffic flow [3].

Our approach involves investigating the “bridge” linking the microscopic description of traffic in terms of particle trajectories with the macroscopic description in terms of viscous fluid flows. Given the trajectory of a particle, we note that the “roughness” or degree of differentiability of the microscopic trajectories bears a well-understood relation to the spread or evolution of the probability density function for the corresponding partial differential equation. The scaling of the mean squared displacement  $\langle x^2 \rangle$  with time  $t$  of a fractal trajectory defines the Hurst exponent  $H$  via the relation  $\langle x^2 \rangle \sim t^{2H}$  [11–13, 16, 17]. The exponent  $H$  uniquely defines the scaling of higher moments of the displacement for monofractal random walks. In contrast, multifractal [12, 13, 15–17] random walks have nonunique scaling exponents. Specifically, one Hurst exponent does not suffice to characterize the scaling of other moments of the displacement of the walker, e.g., the kurtosis. Hölder exponents quantify the number of continuous derivatives that exist along a trajectory and bear a

well-known relation to Hurst exponents [12, 13, 15–17]. Since Hurst exponents depend on averaged quantities, hence only on the probability density function for the random walker, this fact motivates us to study the generalized Hurst and local Hölder exponents in the context of nonlinear convective-diffusive hydrodynamic equations governing vehicle densities in traffic flows. The term “multifractal” refers usually to trajectories, so we also use the more general term “multiscaling” in other contexts.

Hydrodynamic models of traffic describe the vehicle kinematics in terms of a spatial vehicle density field  $\rho(x, t)$  and a velocity field  $v(x, t)$ . The conservation of the number of vehicles may be expressed by a continuity equation

$$\frac{\partial \rho}{\partial t} + \frac{\partial j}{\partial x} = 0, \quad (1)$$

with flux  $j = \rho v - D \nabla \rho$ . The Fickian term is introduced to account for external noise, i.e., the resultant of all random fluctuations in road conditions, drivers' response to stimuli, changes in wind, engine power, braking variability, etc. In independent pioneering studies, Lighthill and Whitham on the one hand and Richards on the other proposed a model of traffic flow [3] that assumes that the velocity  $v$  depends only on the local traffic density:

$$v(x, t) = v(\rho(x, t)). \quad (2)$$

We refer to this model henceforth as the Lighthill-Whitham-Richards (LWR) model. The model can be linearly mapped onto Burger's equation [18] under certain conditions. Being continuity equations, the Burger's and LWR equations conserve the convected-diffused quantity. This model was the first macroscopic (i.e., hydrodynamic) traffic model of the behavior of microscopic self-propelled particles. Although the model has since been considerably improved, it is still used in on-line control applications. It is particularly suited

for the purpose of our investigation due to its relationship with Burger's equation.

We briefly review Burger's equation [18], since it plays a fundamental role in nonlinear convective problems ranging from gas dynamics [19,20] and fluid mechanics [18,21–23] to traffic flow [1,3–5]. It appears naturally whenever the velocity of a convected quantity itself depends linearly on the convected quantity. Shocks and discontinuities are often described in terms of the so-called inviscid Burger's equation, as the prototypical nonlinear hyperbolic partial differential equation [18]. For example, the close relation of the ubiquitous Kardar-Parisi-Zhang (KPZ) equation to the Burger's equation is clear from the fact that, if noise is omitted from the former, the spatial derivative of the KPZ observable obeys, exactly, the Burger's equation [16,24]. Similarly, Burger's turbulence [22,23] has become a benchmark for numerical studies of hydrodynamics.

The standard (parabolic viscous) Burger's equation is a nonlinear convection-diffusion equation, the nonlinearity residing in the convective term. In one dimension this field equation takes the form

$$\frac{\partial u}{\partial t} + u \frac{\partial u}{\partial x} = D \frac{\partial^2 u}{\partial x^2}, \quad (3)$$

for the field  $u(x, t)$ , where  $D$  is the diffusion constant. One of the advantages of the viscous Burger's equation is that it can be mapped via the Cole-Hopf transformation [25],

$$u(x, t) = -2D \frac{\partial}{\partial x} \ln \varphi(x, t), \quad (4)$$

onto the well-known and exactly solvable linear diffusion equation,

$$\frac{\partial \varphi}{\partial t} = D \frac{\partial^2 \varphi}{\partial x^2}. \quad (5)$$

The Cole-Hopf transformation leads to the general solution

$$u = -2D \frac{\partial}{\partial x} \ln \frac{\int_{-\infty}^{\infty} dx' \exp\left(\frac{-(x-x')^2}{4Dt} - \frac{1}{2D} \int_0^{x'} dx'' u_0(x'')\right)}{\sqrt{4\pi Dt}} \quad (6)$$

where  $u_0(x) = u(x, 0)$  is the initial condition.

In this investigation, we apply the formalism of Hurst and Hölder exponents to study solutions of Burger's equation and the LWR model. In Sec. II we briefly review the formalism of the Hurst and Hölder exponents. The application of these concepts and methods to study random walks governed by linear Fokker-Planck equations is straightforward; however, for nonlinear equations the formalism must be carefully generalized. Because the principle of superposition breaks down for nonlinear systems, initial conditions become important; propagators or Green's functions do not exist. In Sec. III we consider  $\delta$ -function initial conditions for Burger's equation. We show that a random walker starting at the origin whose probability density satisfies an equation that can be linearly mapped onto Burger's equation leads to normal monofractal diffusion with  $H=1/2$  (but with a non-Gaussian probability

density). The diffusion part of Burger's equation ensures this behavior. In Sec. IV we consider Burger's equation with other initial conditions and show that they can lead to transient multiscaling. In Sec. V we study the Lighthill-Whitham-Richards hydrodynamic model of traffic. The diffusion constant, the speed limit, and even drivers' reaction time affect the multiscaling. Our results lead to an empirically verifiable prediction: traffic moving from small to large roads becomes locally and temporarily more multifractal near the junction.

## II. FORMALISM

### A. Local Hölder and generalized Hurst exponents

A number of methods can be applied to quantify different aspects of anomalous diffusion. They include continuous-time random walks [26,27], generalized master equations [28], and a variety of other non-Markovian as well as Markovian (subdiffusive and superdiffusive) stochastic approaches, e.g., those with time-dependent diffusion constants, exponential memory, power law memory, and nonlocal effects in space and time [29]. Another formalism, viz. fractional partial differential equations [30,31], can describe anomalous diffusion [31] in the large-time limit.

The particular approach we choose in this paper is the empirically motivated formalism of generalized Hurst exponents. Hurst exponents calculated from the propagator for a random walker not only quantify the type of diffusion, but in their generalized form they allow the estimation via a Legendre transformation of the Hölder exponents [15,17] for the trajectories. The local Hölder exponent for a random walk describes the degree of differentiability along the trajectories. Moreover, this formalism allows us to study the multifractal singularity spectra, i.e., the fractal or Hausdorff dimension  $f(\alpha)$  of the subset of the trajectories with Hölder exponent  $\alpha$  [12,13,16,17].

We briefly describe the formalism and methodology. Following convention [5,16,17], we define the generalized Hurst exponent  $H(q)$  for a stationary stochastic process in terms of the scaling of the absolute moments of the density:

$$\bar{x} \equiv \langle x \rangle, \quad (7)$$

$$M_q(t) \equiv \langle |x - \bar{x}|^q \rangle \sim t^{qH(q)}, \quad (8)$$

where the averages are taken over the propagator or the probability density function for a single random walker. Normal diffusion corresponds to  $H(q) = H = 1/2$ , whereas anomalous diffusion corresponds to all other cases.

Moreover, we can further generalize the concept to allow a time or scale dependence [32–34], such that  $H = H(q, t)$ :

$$\langle |x - \bar{x}|^q \rangle \sim t^{qH(q,t)}. \quad (9)$$

This generalization allows the treatment of phenomena whose behavior depends on the time scale being studied. Consider, as an illustrative example, the telegrapher's equation [35]. The mean squared displacement grows quadratically for small times and then becomes linear for larger times. So the behavior is ballistic at small times,  $H(q, t) \approx 1$ .

However, it is diffusive at large times, i.e.,  $H(q, t) \rightarrow 1/2$ . Hence, this time (or scale) dependence is a restatement of the well-known fact that the diffusive properties (or equivalently, the roughness) of the trajectories do in fact depend on the scale at which one studies them.

The generalized Hurst exponent  $H(q)$  bears a relation to the local Hölder exponent  $\alpha$  via the following Legendre transform:

$$\alpha = \frac{d}{dq} [qH(q) - 1], \tag{10}$$

$$f(\alpha) = q\alpha - [qH(q) - 1]. \tag{11}$$

Here,  $f$  gives the Hausdorff or fractal dimension of the subset of the series characterized by the Hölder exponent  $\alpha$ . The literature also refers to  $\alpha$  as the singularity strength [5,15,17]. The value of  $\alpha$  represents a measure of the number of continuous derivatives that the underlying trajectory possesses. The singularity spectrum of monofractal random walks will show a unique Hölder exponent, while a multifractal series will show a range of values for  $\alpha$ .

Here we use a further generalization of the concept of the singularity spectrum that relaxes the condition of taking the small scale limit to compute  $\alpha$ . Instead, we follow an empirically motivated approach that takes into account the fact that one cannot experimentally observe arbitrarily small or large scales of time or space. Empirically estimated multifractal spectra, Hurst exponents and Hölder exponents do in fact all depend on the range of scales being investigated [32–34].

Finally, note that monofractality does not imply  $H=1/2$ ; for example, fractional Brownian motion is monofractal with  $H(q)=H$ , but the diffusion is anomalous, i.e.,  $H \neq 1/2$  [12].

**B. Langevin, Fokker-Planck and hydrodynamic perspectives**

In this work we estimate the Hurst exponents not from actual trajectories but rather by inferring them from the behavior of the density distribution  $\rho(x, t)$ . Realizing that the nonlinearity of hydrodynamic traffic models precludes propagators, we briefly discuss, in a larger context [36], the passage from the Langevin to the Fokker-Planck descriptions.

If the nonstochastic forces that act on  $N$  identical interacting random walkers depend only on the positions of the other walkers, then we can always express the trajectories via coupled Langevin equations:

$$\dot{x}_i = F_i(\{x_j\}) + \xi_i(t), \tag{12}$$

where  $F_i$  represent smooth forces (which can depend on the positions) and  $\xi$  the noise. The  $N$ -particle probability density function  $P(x_i)$  will then satisfy a linear Fokker-Planck equation of the form

$$\dot{P}(x_i) = LP(x_i), \tag{13}$$

which is linear in that the operator  $L$  does not depend on  $P$ . This is a crucial point: the standard methods of deriving Fokker-Planck equations from Langevin equations lead al-

ways to linear equations. In this context, Burger’s equation, if interpreted similarly to a Fokker-Planck equation, is different since its  $L$  does depend on  $P$ .

The situation can be understood through a comparison to the Boltzmann equation for gases, obeyed by the one-molecule distribution function, which is nonlinear, in contrast to the underlying linear Liouville equation for the  $N$ -molecule Liouville density. In the absence of intermolecular interactions, the Boltzmann equation would be trivially linear. If the gas molecules were to interact with a fixed system of random scatterers, the Boltzmann equation would be nontrivial but still linear. The standard manner of applying Hurst and Hölder exponents would work here. If intermolecular interactions were turned on, however, nonlinearity would enter immediately, making unavailable superposition and propagator analysis.

This means that we need here a method that generalizes and extends the formalism of Hurst exponents to nonlinear convective-diffusive equations. We recall the standard manner in which the Hurst exponent  $H=H(2)$  is usually obtained from the behavior of the mean squared displacement for linear equations. In terms of the propagator or the Green function  $\psi(x, x_0, t)$ , the Hurst exponent is given by the scaling behavior of

$$\int_{-\infty}^{\infty} \int_{-\infty}^{\infty} dx dx_0 (x - x_0)^2 \psi(x, x_0, t) \rho(x_0),$$

which, for a translationally invariant (homogeneous) system such as the one under consideration in this paper, reduces to

$$\langle x^2 \rangle_{\delta} = \int dx x^2 \psi(x, t) \tag{14}$$

because the propagator is a function of the difference  $x - x_0$ . We use the suffix  $\delta$  in the left-hand side of Eq. (14) to emphasize that the  $\langle x^2 \rangle$  used here can be considered to be the one calculated for an initially localized initial condition  $\rho_0(x_0) = \delta(x_0)$ . This can also be used for a collection of many random walkers provided they are noninteracting among themselves: the initial density  $\rho_0$  is irrelevant in a linear system of noninteracting particles.

However, when the particles interact such that the density  $\rho$  satisfies a nonlinear equation, the nonlinearity prevents us from making use of

$$\rho(x, t) = \int_{-\infty}^{\infty} dx_0 \rho_0(x_0) \psi(x - x_0, t),$$

which is no longer valid. The most natural generalization to be used for an extended approach of Hurst exponents is to compute  $\langle x^2 \rangle_{\rho_0}$  by substituting  $x_0$  with the center  $\bar{x}_0$  of the distribution at time  $t=0$ :

$$\langle x^2 \rangle_{\rho_0} = \int_{-\infty}^{\infty} dx (x - \bar{x}_0)^2 \rho(x, t, \rho_0), \tag{15}$$

where  $\rho$  now depends nonlinearly on  $\rho_0$ . The crucial point to notice is that we can no longer expect  $\langle x^2 \rangle_{\rho_0}$  to remain independent of  $\rho_0$ . The same holds true for other moments  $\langle |x|^q \rangle$ .

In this context, multiscaling of solutions to nonlinear convective-diffusive equations has a clear interpretation. If  $\rho$  “widens” but retains the same functional form (under rescalings), then the variance  $\langle x^2 \rangle - \langle x \rangle^2$  alone suffices to describe the diffusion, i.e.,  $H(q)=H$ . On the other hand, if the shape or functional form of  $\rho$  changes, then a single Hurst exponent is not sufficient to describe the scaling. The interpretation is thus identical to what is well known for propagators of linear equations. The main difference is that we can no longer ignore initial conditions.

### III. RANDOM WALK STARTING AT THE ORIGIN SATISFYING BURGER’S EQUATION

Consider a single random walker starting at the origin whose probability density function  $p(x,t)$  evolves according to Burger’s equation, i.e.,  $p(x,t)=u(x,t)$ . The solution of Eq. (1) when the initial condition is a  $\delta$  function centered around the origin i.e.,  $u(x,t=0)=A\delta(x)$ , is

$$u(x,t) = \sqrt{\frac{4D}{\pi t}} \left( \frac{(e^{A/2D} - 1)e^{-x^2/4Dt}}{1 + e^{A/2D} + (1 - e^{A/2D})\phi(x/\sqrt{4Dt})} \right). \quad (16)$$

Here  $\phi$  is the error function.

Noting that  $u(x,t)$  is of the form  $u(x,t)=n(t)g(x^2/t)$ , we can easily show that  $\langle x^{2n} \rangle \sim t^n$ ; hence  $H(q)=1/2$  for all  $q$ . Similarly, we can show straightforwardly that this result extends to all cases where  $p(x,t)=F[u(x,t)]$  where  $F$  is some function. In all such cases the underlying random walk trajectory is monofractal with  $H=1/2$  [despite  $p(x,t)$  not being Gaussian].

Notice that if we interpret  $u(x,t)$  not as the probability density function, but rather as the density  $\rho(x,t)$  for a collection of particles, we obtain the same result,  $H(q)=1/2$ , for the  $\delta$ -function initial condition  $\rho_0(x)=\delta(x)$ . In this context, the LWR model does not provide information about the single-particle probability density function, rendering impossible the investigation of trajectories of a single vehicle. Yet we can still reach the conclusion that  $H(q)=1/2$  for the individual trajectories, due to the special nature of the  $\delta$ -function initial condition. Although  $u(x,t)$  in Eq. (16) is not a propagator, it shares certain similarities.

This monofractal normal diffusion for the  $\delta$ -function initial condition is due to the relation, via the Cole-Hopf transformation, to the diffusion equation and to the fact that, in multifractal random walks, the probability density function changes shape (i.e., its functional form), rather than just widening as time evolves. An important point to note is that, for large enough times, solutions with any initial condition with compact support will converge asymptotically to an identical functional form. This limiting functional form is none other than Eq. (16). This convergence guarantees  $H(q)=1/2$  for large enough times. Another way of stating the same fact is that the diffusion term in the Burger’s equation containing the Laplacian operator dominates over the nonlinear convection. As the particles diffuse, the peak local densities decrease—thereby weakening the nonlinear convection that is proportional to the local densities.

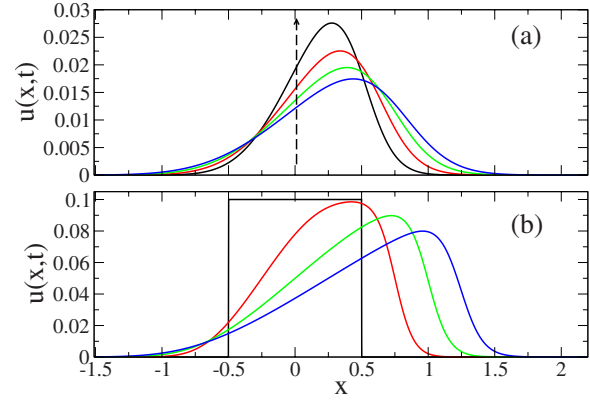


FIG. 1. (Color online) Illustrative examples of solutions of the Burger’s equation at successive times where the initial condition is (a) a  $\delta$  function at the origin and (b) a square pulse of unit width.

### IV. BURGER’S EQUATION: DEPENDENCE ON INITIAL CONDITIONS

We can expect that for different initial conditions the time necessary to dissipate (initial) structures may be sufficiently large so as to allow multiscaling at given time scales. To illustrate this point we study the solution of the Burger’s equation when the initial condition corresponds to a square pulse function of the form

$$u(x,t=0) = \begin{cases} 0, & x < L_1, \\ f, & L_1 < x < L_2, \\ 0, & L_2 < x. \end{cases} \quad (17)$$

The solution is found to be

$$u(x,t) = \frac{f\chi e^{f(L_1-x+ft)/2D}}{1 + \phi(L_1) + e^{f(L_1-L_2)/2D}(1 - \phi(L_2)) + \chi e^{f(L_1-x+ft)/2D}}, \quad (18)$$

where

$$\phi(L_i) = \phi\left(\frac{L_i - x}{\sqrt{4Dt}}\right), \quad (19)$$

$$\chi = \chi(x,t) = \phi\left(\frac{L_2 - x + ft}{\sqrt{4Dt}}\right) - \phi\left(\frac{L_1 - x + ft}{\sqrt{4Dt}}\right), \quad (20)$$

and  $\phi(x)$  is the well-known error function  $\text{erf}(x)$ .

Figure 1 shows the time evolution of solutions to the Burger’s equation for two initial conditions: in Fig. 1(a) a  $\delta$  function centered at the origin and in Fig. 1(b) a square pulse also centered at the origin. Figure 2 shows the Hurst exponents calculated from Eq. (9). For the  $\delta$  function, we find that  $H(q)=1/2$  for all  $q$ , as expected from Eq. (16). In contrast, we see multiscaling behavior for the square pulse. Figure 2(b) shows this multiscaling more clearly: for the square pulse,  $H(q)$  increases with  $q$ .

Figure 3 shows how the solutions corresponding to the two initial conditions behave under rescalings of the form  $u \rightarrow u/u_{\max}(t)$ ,  $x \rightarrow \lambda x$ , where  $\lambda$  is some dilation factor and  $u_{\max}$  is the maximum or peak value of  $u$ . We can see in Fig.

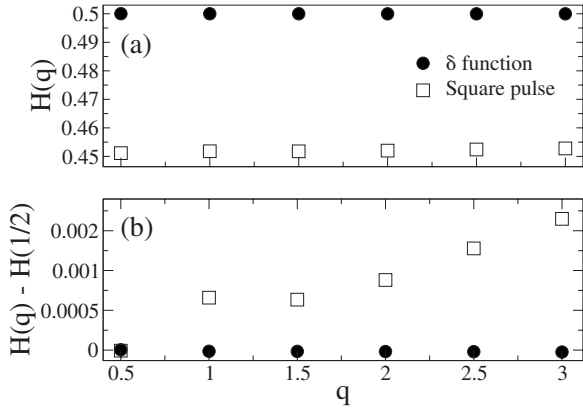


FIG. 2. Generalized Hurst exponents  $H(q)$  estimated for  $\delta$ -function and square pulse initial conditions. They are shown in (a) directly and in (b) after subtracting the initial value  $H(q=1/2)$ . The Hurst exponents for the  $\delta$ -function initial condition not only are closer to the theoretical value for random walks,  $H=1/2$ , but they do not vary with  $q$ . In contrast, (b) shows multiscaling behavior for the square pulse initial condition. We have used a value of the diffusion constant  $D=0.04$  (here and elsewhere in the paper we express  $D$  in arbitrary units) and estimated  $H(q)$  for  $3 \leq \ln t \leq 3.2$ .

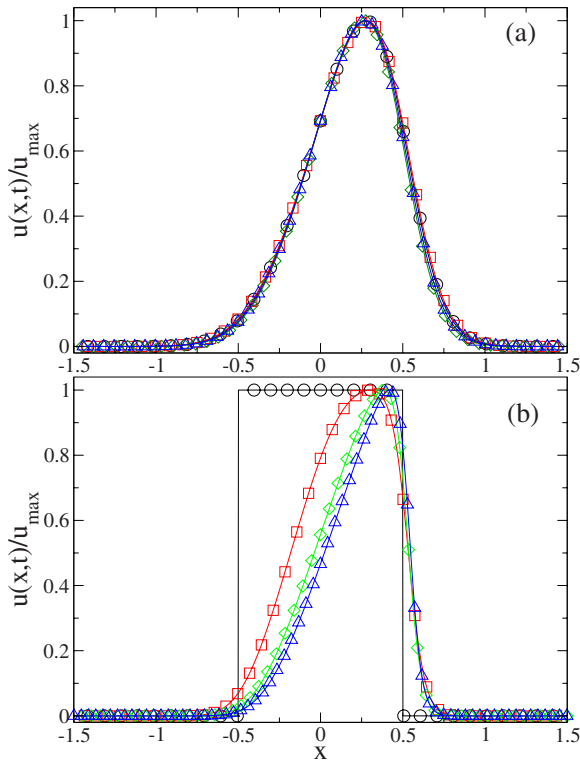


FIG. 3. (Color online) Rescaled plots of the data shown in Fig. 1 (see text). Notice that the  $\delta$ -function initial condition leads to a solution that maintains the same functional shape (a). In contrast, the square pulse deforms and does not retain the same functional form (b). The data collapse seen for the  $\delta$  function does not happen for the square pulse initial condition except for relatively large time scales. These shape deformation effects lead to multiscaling at small enough time scales.

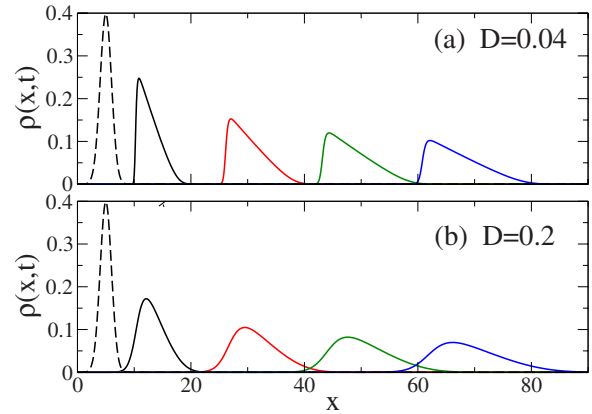


FIG. 4. (Color online) Illustrative examples of solutions of the LWR model of traffic flow using Eq. (21). Plots show the vehicle density at successive times for (a) smaller diffusion constant  $D=0.04$  and (b) larger diffusion constant  $D=0.2$ , for identical Gaussian initial conditions (dashed line) with  $\rho_j=1$ ,  $v_0=1$ . For small diffusion constants, the nonlinear effects of velocity-dependent convection become more prominent and hence more important.

3(a) that the solutions corresponding to the initial  $\delta$  function rescale, whereas we find no data collapse for the solutions corresponding to the initial square pulse, Fig. 3(b). As mentioned earlier, a prerequisite for multifractality and multiscaling is that the density should not merely rescale (or widen) but must deform and change its functional form, as seen for the square pulse.

The above findings demonstrate that nonlinear convection can lead to transient multiscaling. In what follows, we study this phenomenon in a specific physical system of self-propelled particles that in certain circumstances can be mapped to a Burger’s equation.

V. MULTISCALING ANALYSIS OF THE LWR MODEL

In this section we analyze the scaling of the solutions of LWR model. A popular choice [37] for  $v$ , based on experimental observations is

$$v(x,t) = v_0 \left( 1 - \frac{\rho(x,t)}{\rho_j} \right), \tag{21}$$

where  $v_0$  is the maximum or free flow speed and  $\rho_j$  represents the critical jam density. The free flow speed is the speed at which a single vehicle moves in an otherwise empty road. The jam density is the density at which the traffic stops completely. For a Gaussian initial condition, it is much easier to find the solutions numerically in practice. In all subsequent figures, the solutions are numerically evolved with a time discretization step (i.e., increment) of  $\Delta t=0.005$ . Figure 4 shows how the LWR model behaves, with more dense regions of traffic moving more slowly than lower-density regions.

A. Dependence on the diffusion constant

One can show that the LWR model yields a Burger’s equation,

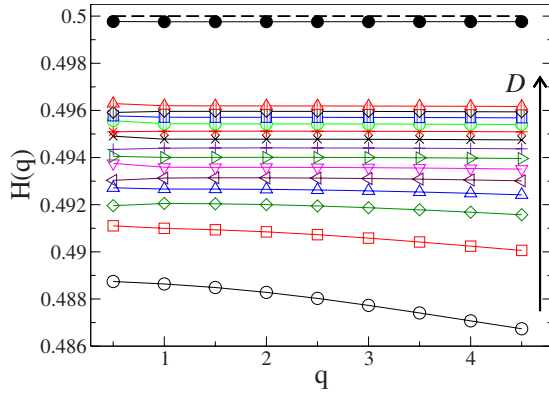


FIG. 5. (Color online) Generalized Hurst exponents  $H(q)$  for identical Gaussian initial conditions with  $\rho_j=2$ ,  $v_0=0.1$  for various diffusion constants in the order indicated by the arrow:  $D=0.004, 0.008, 0.012, 0.016, 0.02, 0.024, 0.028, 0.032, 0.036, 0.04, 0.044, 0.048, 0.052, 0.056$ , and  $0.2$  (filled circles). The values  $H(q)$  were estimated for  $4 \leq \ln t \leq 6$ . Note how the curves become essentially flat for large  $D$ , with  $H(q) \rightarrow H=1/2$  (dashed line).

$$\frac{dr}{dt} + r \frac{dr}{dx} = D \frac{d^2 r}{dx^2}, \quad (22)$$

with  $r(x, t) = v_0(1 - 2\rho/\rho_j)$ . We solve numerically the LWR model for the case in which the initial density  $\rho_0$  is a Gaussian centered in the origin. The dependence of the degree of inferred multifractality with the diffusion constant  $D$  is sum-

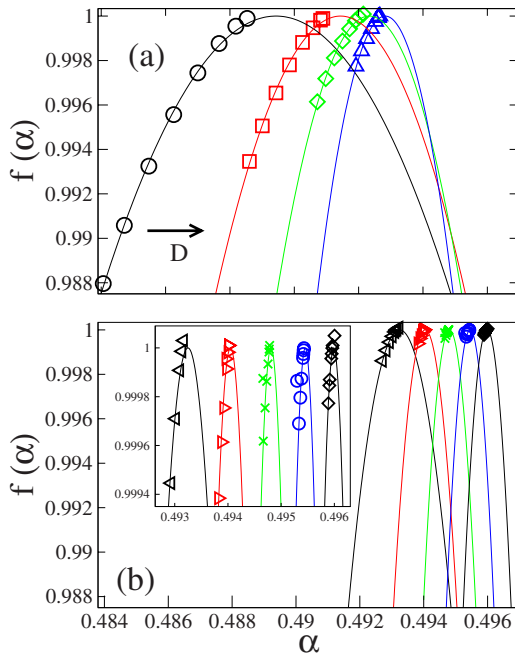


FIG. 6. (Color online) Fractal dimension  $f(\alpha)$  for subset with Hölder exponents  $\alpha$  estimated from the data shown in Fig. 5. Here the Hurst exponents have been interpreted as if they were estimated from actual trajectories. The spectra are shown in two panels with the same scale to avoid clutter. The inset shows a zoom of the second panel. For small diffusion constants, the velocity-dependent advection effects lead to transient multiscaling.

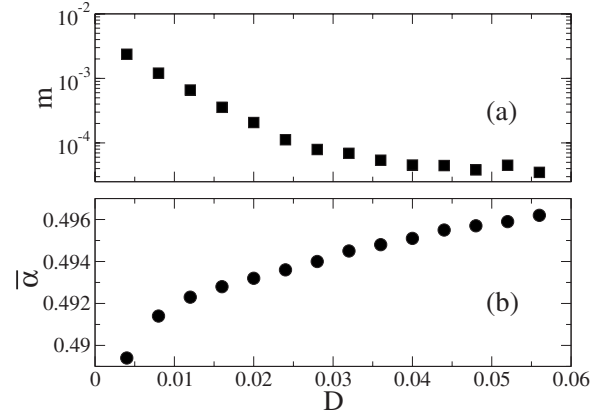


FIG. 7. (a) Degree of multifractality  $m$  and (b) central Hölder exponent  $\bar{\alpha}$  for the data shown in Fig. 6. The value of  $m$  is calculated as the inverse of the quadratic coefficient of the parabolic fits for  $f(\alpha)$ , while  $\bar{\alpha}$  is the value of the maximum of  $f(\alpha)$ . As  $D$  increases, the inferred multifractality clearly decreases, and the  $\bar{\alpha}$  approaches  $H=1/2$  as expected.

marized in Fig. 5, showing how the Hurst exponents depend on  $D$ . Figure 6 shows inferred singularity spectra estimated from the Hurst exponent. The width of the singularity spectra indicates the degree of multifractality. A wide curve shows multifractality, whereas a very narrow curve shows approximate monofractal scaling. The maximum in  $f(\alpha)$  shows the dominant  $\alpha$ . Figure 7 shows how the degree or strength of the multifractality depends on the  $D$ . The degree of inferred multifractality decreases as the diffusion constant  $D$  increases.

**B. Dependence on the free flow velocity**

Figure 8 shows  $H(q)$  and Fig. 9 shows the inferred singularity spectra estimated from the generalized Hurst exponents. On the one hand, a larger free flow velocity  $v_0$  leads to Hurst exponents closer to  $1/2$ . This can be seen from the fact that the centers of the spectra shift toward  $\alpha=1/2$  for larger  $v_0$ . On the other hand, the degree of multifractality (i.e., the width of the spectra) actually increases.

The likely explanation for this unexpected result is that a larger  $v_0$  leads to a more rapid deformation of the “shape”

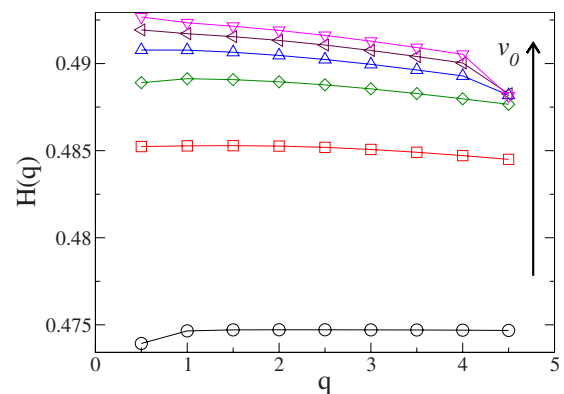


FIG. 8. (Color online)  $H(q)$  for  $v_0=0.1, 0.3, 0.5, 0.7, 0.9, 1.1$  for identical initial conditions ( $D=0.02$ ).

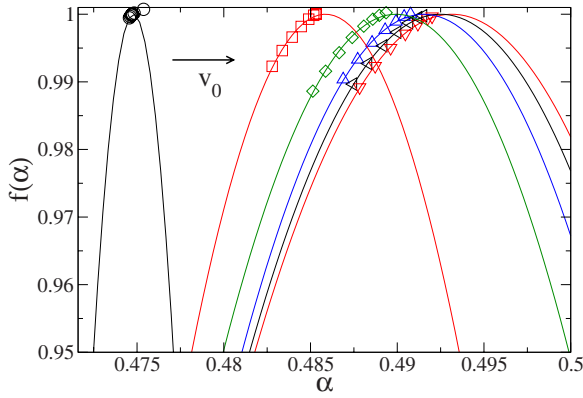


FIG. 9. (Color online) Fractal dimension  $f(\alpha)$  for subset with Hölder exponents  $\alpha$  for  $v_0=0.1, 0.3, 0.5, 0.7, 0.9, 1.1$  for identical initial conditions. On the one hand, the inferred singularity spectra become wider, i.e., more multifractal, for larger  $v_0$ . On the other hand, the centers of the spectra approach  $\alpha=1/2$ . Hence, increasing the nonlinear convection via larger free flow velocities leads to unexpected phenomena.

(the functional form) of the density function for fixed initial condition, jam density, and diffusion constant. This more rapid nonlinear convection leads to greater multiscaling (hence, to inferred multifractality). However, this more rapid nonlinear convection leads to greater excitation of higher-spatial-frequency modes in the Fourier domain, which are

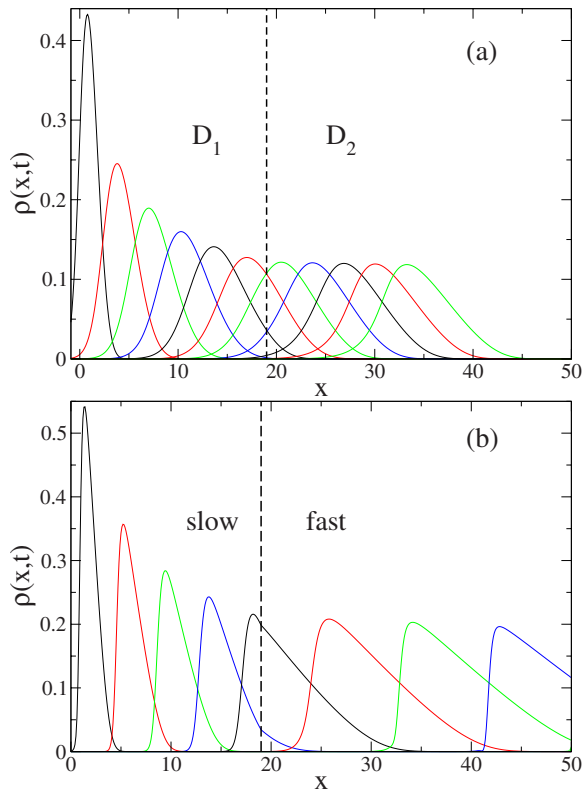


FIG. 10. (Color online) Illustrative example of a traffic wave that moves from a region of (a) larger to smaller diffusion constant ( $D_1=0.5, D_2=0.05, v_0=2$ ), and (b) smaller to larger free flow velocity ( $v_{01}=1, v_{02}=2, D=0.05$ ). In both cases the change occurs at  $x=X=19$ .

damped at a rate proportional to the square of the spatial frequency. Hence, the convergence to  $H=1/2$  also proceeds more quickly.

These findings clearly demonstrate the nontrivial nature of the interaction between the diffusive and convective aspects of the LWR model. Nonlinear convective-diffusive phenomena can give rise to remarkably rich phenomenology.

### C. Traffic flow from dirt roads to highways

In general, minor roads have lower-quality pavement and more traffic lights than highways. This means that they can be represented by larger diffusion constants. For similar reasons, the speed limit is smaller than the one on a major highway. In this section we investigate how these factors affect the behavior of traffic moving from minor to major roads. This is done by assuming that in the LWR model the diffusion constant, or the free flow velocity, changes at some point along the road i.e.,  $D_1$  for  $x < X$  and  $D_2$  for  $x > X$ , and similarly for  $v_0$ . Figure 10 shows how the traffic density is affected by changes in  $D$  [Fig. 10(a)] and  $v_0$  [Fig. 10(b)] along the road.

Figure 11 shows the behavior of a traffic wave moving from a region of large diffusion constant to one with a smaller diffusion constant. The main finding is that there is a sudden local spike in the degree of multiscaling (or inferred multifractality). Figure 12 shows the analogous result for free flow velocity. Both effects can increase multiscaling near the junction of the two regions. We find that as the traffic moves into the highway, there is a local, temporary

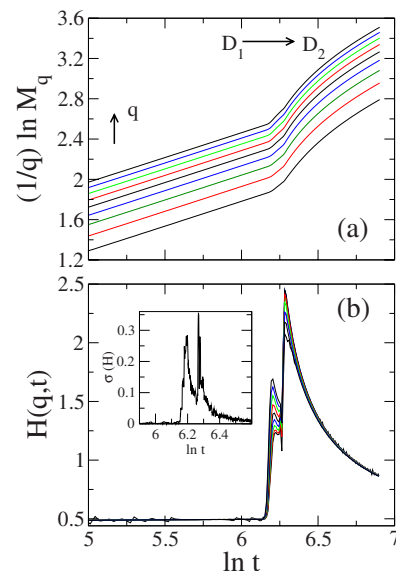


FIG. 11. (Color online) (a) Double logarithmic plot of the  $q$  root of the moments versus time for the case where the traffic wave propagates from a region of high to low diffusion constant, such as might happen when vehicles move from back alleys to major highways. (b)  $H(q)$  estimated as the local slope of the curves shown in (a). Inset shows the standard deviation of  $H(q,t)$  over nine values of  $q$  ( $q=i/2, i=1-9$ ). There is a sudden spike in multiscaling that occurs when the traffic wave goes from one region to the other, which subsequently decays.  $D_1=0.5, D_2=0.05, v_0=2$ .

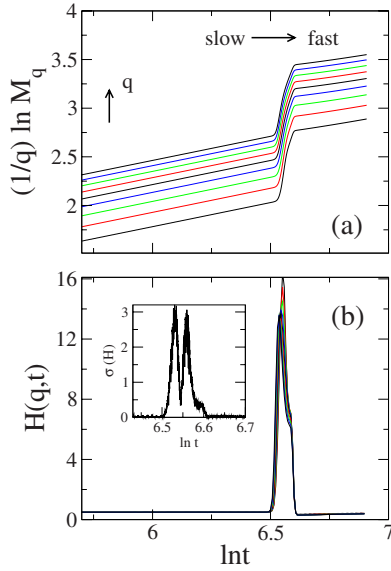


FIG. 12. (Color online) (a) Double logarithmic plot of the moments and (b) Hurst exponents corresponding to the ones in Fig. 11, for the case where the traffic wave propagates from a region of low to high free flow velocity, such as might happen when vehicles move from back alleys to major highways. Inset shows the standard deviation of  $H(q)$ , as in Fig. 11. There is again a similar sudden spike in the apparent multiscaling near the junction ( $v_{01}=1$ ,  $v_{02}=2$ ,  $D=0.05$ ).

increase in anomalous diffusion effects, due to the increase in  $v_0$  and decrease in  $D$ .

**D. Time delays due to reaction time**

A driver’s reaction time is an important factor to be considered in any realistic model of traffic. A simple way to incorporate such time-delay effects in the LWR model is by assuming that the velocity reaches equilibrium within some relaxation time, such that  $v(x,t)=v(\rho(x,t-\tau))$ . Then the LWR equation for the density takes the form

$$\frac{\partial \rho}{\partial t} + v_0 \left( 1 - \frac{\rho'}{\rho_j} \right) \frac{\partial \rho}{\partial x} - v_0 \frac{\rho}{\rho_j} \frac{\partial \rho'}{\partial x} = D \frac{\partial^2 \rho}{\partial x^2}, \quad (23)$$

where  $\rho=\rho(x,t)$  and  $\rho'=\rho(x,t-\tau)$

We have solved numerically the above equation with the same initial conditions selected to study the standard LWR model. The first interesting result that we find is that the density (and therefore the velocity) show distinctive spatial patterns that disappear at large times (Fig. 13).

An analysis of the results indicates that the time delay leads to deviations from monofractal behavior. The change in the functional form of the density as time evolves guarantees that the moments grow in a nontrivial manner, hence multiscaling is expected (Fig. 14). So, in addition to the effects of  $v_0$  and  $D$ , yet another potential source of multifractality is the reaction time of the driver. However, we have yet to uncover the systematic effects of such time delays; this issue merits further investigation.

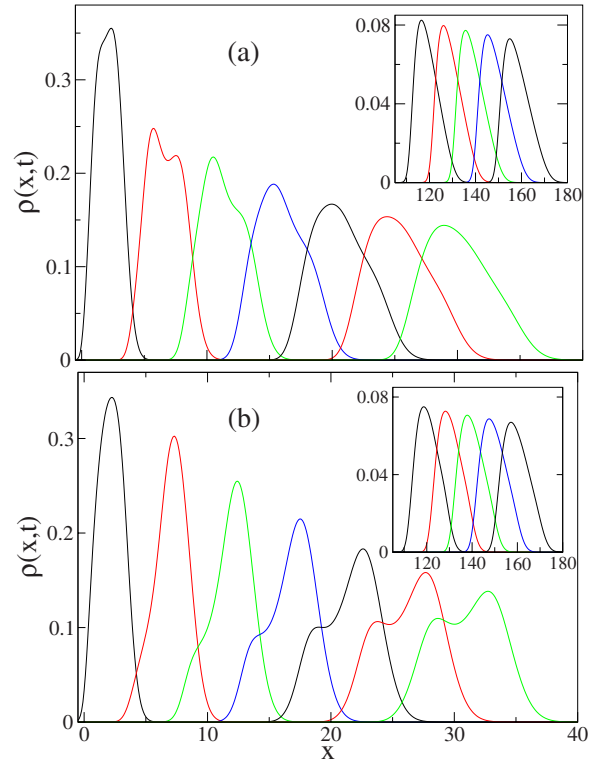


FIG. 13. (Color online) Density function for the LWR model with time delay for different times. The insets indicates the behavior of  $\rho$  at longer times.  $\tau=(a)$  3 and (b) 6. The data were obtained for  $D=0.02$ ,  $\rho_j=2$ ,  $v_0=0.5$ ; the time intervals are the same in (a) and (b). At  $t=0$  the density is a Gaussian centered around the origin. Notice that in both cases the spatial patterns disappear at longer times, but take much longer to disappear for the larger  $\tau$ .

**VI. CONCLUDING REMARKS**

With the aim of studying multifractality in traffic, we have extended the formalism of Hurst exponents to the study of diffusion governed by nonlinear partial differential equa-

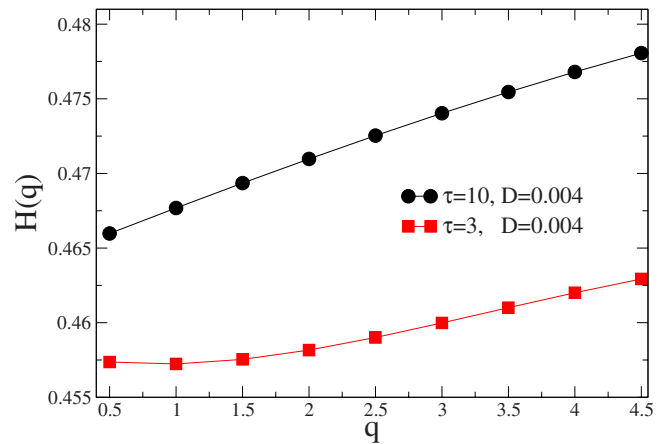


FIG. 14. (Color online)  $H(q)$  for two different time delays and identical parameters  $D$  and  $v_0$  and initial conditions. The multiscaling is due to the evolution of spatial patterns (Fig. 13). The nature of these patterns and their systematic effect merit further investigation.



tions. We have shown that all initial conditions with compact support for Burger's equations and the LWR model lead to monofractal normal diffusion (i.e.,  $H=1/2$ ) in the large-time limit. However, due to the nonlinearity, initial conditions become non-negligible due to the breakdown of the principle of superposition and the consequent nonexistence of propagators. For many initial conditions, a transient multiscaling regime precedes the asymptotic approach to the large time monofractal behavior.

Subsequent to the original interest in Burger's equation arising from the LWR model, some authors have focussed on the noisy Burger's equation [38,39]. A detailed account of this equation can be found in a study by Fogedby [40]. Noise can enter Burger's equation in a non-unique manner. The diffusion term in the viscous Burger's equation accounts for fluctuations that generate Fickian transport. In contrast, the noisy Burger's equation contains an additional input of space- and time-dependent noise which introduces stochasticity directly into the dynamics. For traffic, this extra term adds fluctuations to the flux  $j$  of vehicles. The noisy Burger's equation bears a relation to the Nagel-Schreckenberg (NaSch) cellular automata (CA) model of traffic [39]. Similar CA models appear in surface growth [16,24,41], whose relation to the noisy Burger's equation is well known. The connection between traffic and surface growth is that local particle movement along the road in the NaSch model corresponds to local forward growth of the surface via particle deposition (e.g., see Ref. [2]).

In the context of nonlinear evolution equations for the density, the noisy Burger's equation would correspond to a "noisy" Fokker-Planck equation. Our viewpoint in the present investigation has been to incorporate noise only at the basic Langevin level of the traffic description. With such a viewpoint, in the passage to the Burger's (Fokker-Planck) description, the noise disappears as a random term and appears only as the diffusive term. For this reason, we do not consider here the noisy Burger's equation. However, this topic certainly merits further study in future investigations.

In summary, we have explored how multiscaling and multifractality might arise at given spatial and temporal scales in traffic governed by the LWR model. We have investigated multiscaling in the context of nonlinear waves in traffic and the results reported here suggest that a traffic wave packet that propagates from a slow, high-viscosity region (e.g., minor roads) to a fast, low-viscosity region (e.g., major highway) may appear locally and temporarily more multifractal. This prediction can be empirically tested using data consisting of actual trajectories in traffic.

#### ACKNOWLEDGMENTS

We thank A. Budini, P. Parris, V. Dossetti, and M. G. E. da Luz for helpful discussions. This work was supported in part by NSF Grant No. INT-0336343. G.M.V. acknowledges support from CNPq (Process No. 201809/2007-9).

- 
- [1] D. Helbing, *Rev. Mod. Phys.* **73**, 1067 (2001).  
 [2] D. Chowdhury, L. Santen, and A. Schadschneider, *Phys. Rep.* **329**, 199 (2000).  
 [3] M. J. Lighthill and G. B. Whitham, *Proc. R. Soc. London, Ser. A* **229**, 317 (1955); P. I. Richards, *Oper. Res.* **4**, 42 (1956).  
 [4] D. Ngoduy and R. Liu, *Physica A* **385**, 667 (2007); J. B. Sheu, *ibid.* **367**, 461 (2006); P. Nelson, *Phys. Rev. E* **61**, R6052 (2000); B. S. Kerner, S. L. Klenov, and P. Konhauser, *ibid.* **56**, 4200 (1997); D. Helbing, *Physica A* **219**, 375 (1995); D. Helbing, *Phys. Rev. E* **51**, 3164 (1995).  
 [5] J. Ward, R. E. Wilson, and P. Bergh, *Physica D* **236**, 1 (2007).  
 [6] X. W. Li and P. J. Shang, *Chaos, Solitons Fractals* **31**, 1089 (2007).  
 [7] P. J. Shang, Y. B. Lu, and S. Kamae, *Chaos, Solitons Fractals* **36**, 82 (2008).  
 [8] M. I. Bogachev, J. F. Eichner, and A. Bunde, *Eur. Phys. J. Spec. Top.* **161**, 181 (2008).  
 [9] J. Levy-Vehel and R. Vojak, *Rapport de Recherche No. 1943*, INRIA, France, 1993 (unpublished).  
 [10] A. Kudrolli, G. Lumay, D. Volfson, and L. S. Tsimring, *Phys. Rev. Lett.* **100**, 058001 (2008); F. Peruani and L. G. Morelli, *ibid.* **99**, 010602 (2007); A. Baskaran and M. C. Marchetti, *Phys. Rev. E* **77**, 011920 (2008).  
 [11] H. E. Hurst, R. P. Black, and Y. M. Simaika, *Long-Term Storage: An Experimental Study* (Constable, London, 1965).  
 [12] B. B. Mandelbrot, *The Fractal Geometry of Nature* (W. H. Freeman and Co., New York, 1982).  
 [13] A. Bunde and S. Havlin, *Fractals and Disordered Systems* (Springer, Berlin, 1991).  
 [14] Bruce J. West and William D. Deering, *The Lure of Modern Science: Fractal Thinking* (World Scientific, Singapore, 1995).  
 [15] J. Feder, *Fractals* (Plenum Press, New York, 1988).  
 [16] A. L. Barabási and H. E. Stanley, *Fractal Concepts in Surface Growth* (Cambridge University Press, Cambridge, U.K., 1995).  
 [17] J. W. Kantelhardt, S. A. Zschiegner, E. Koscielny-Bunde, S. Havlin, A. Bunde, and H. E. Stanley, *Physica A* **316**, 87 (2002); C. M. Nascimento, H. B. N. Junior, H. D. Jennings, M. Serva, I. Gleria, and G. M. Viswanathan, *Europhys. Lett.* **81**, 18002 (2008).  
 [18] G. B. Whitham, *Linear and Nonlinear Waves*, Pure and Applied Mathematics Vol. 1237 (Wiley, New York, 1974).  
 [19] J. A. Shercliff, *Rev. Mod. Phys.* **32**, 980 (1960).  
 [20] E. Ben-Naim, S. Y. Chen, G. D. Doolen, and S. Redner, *Phys. Rev. Lett.* **83**, 4069 (1999); P. Carbonaro, *Phys. Rev. E* **56**, 2896 (1997).  
 [21] P. Constantin and C. Foias, *Navier-Stokes Equations*, Chicago Lectures in Mathematics Vol. 19 (University Of Chicago Press, Chicago, 1989).  
 [22] W. A. Woyczynski, *Burgers-KPZ Turbulence: Göttingen Lectures*, Lecture Notes in Mathematics (Springer, Berlin, 1999).  
 [23] *Nonlinear Stochastic PDE's: Hydrodynamic Limit and Burgers' Turbulence*, edited by T. Funaki and W. A. Woyczynski, The IMA Volumes in Mathematics and its Applications

- (Springer, Berlin, 1995).
- [24] M. Kardar, G. Parisi, and Y. C. Zhang, *Phys. Rev. Lett.* **56**, 889 (1986).
- [25] E. Hopf, *Pure Appl. Math.* **3**, 201 (1950); J. D. Cole, *Q. Appl. Math.* **9**, 225 (1951).
- [26] E. W. Montroll and G. Weiss, *J. Math. Phys.* **6**, 167 (1965).
- [27] H. Scher and M. Lax, *Phys. Rev. B* **7**, 4491 (1973); H. Scher and E. W. Montroll, *ibid.* **12**, 2455 (1975).
- [28] V. M. Kenkre, in *Statistical Mechanics and Statistical Methods in Theory and Application*, edited by U. Landman (Plenum, New York, 1977); V. M. Kenkre, E. W. Montroll, and M. F. Shlesinger, *J. Stat. Phys.* **9**, 45 (1973).
- [29] V. M. Kenkre and F. J. Sevilla, in *Contributions in Mathematical Physics*, edited by S. T. Ali and K. B. Sinha (Hindustan Book Agency, New Delhi, 2007).
- [30] E. Barkai, R. Metzler and J. Klafter, *Phys. Rev. E* **61**, 132 (2000).
- [31] R. Metzler and J. Klafter, *Phys. Rep.* **339**, 1 (2000); R. Metzler and J. Klafter, *J. Phys. A* **37**, R161 (2004).
- [32] Y. S. Ji, *IEICE Trans. Commun.* **E89-B**, 2125 (2006).
- [33] R. L. Costa and G. L. Vasconcelos, *Physica A* **329**, 231 (2003).
- [34] G. M. Viswanathan, S. V. Buldyrev, S. Havlin, and H. E. Stanley, *Physica A* **249**, 581 (1998); G. M. Viswanathan, S. V. Buldyrev, S. Havlin, and H. E. Stanley, *Biophys. J.* **72**, 866 (1997); G. M. Viswanathan, C. K. Peng, H. E. Stanley, and A. L. Goldberger, *Phys. Rev. E* **55**, 845 (1997).
- [35] V. M. Kenkre, in *Modern Challenges in Statistical Mechanics: Patterns, Noise and the Interplay of Nonlinearity and Complexity*, Proceedings of the Pan American Advanced Studies Institute, Bariloche, Argentina, edited by V. M. Kenkre and K. Lindenberg (AIP, Melville, NY, 2003).
- [36] Katja Lindenberg and Bruce J. West, *The Nonequilibrium Statistical Mechanics of Open and Closed Systems* (VCH, New York, 1990).
- [37] D. L. Gerlough and M. J. Huber, Transportation Research Board Special Report No. 165, National Research Council, Washington, DC, 1975 (unpublished).
- [38] D. Forster, D. R. Nelson, and M. J. Stephen, *Phys. Rev. A* **16**, 732 (1977); T. Musha and H. Higuchi, *Jpn. J. Appl. Phys.* **17**, 811 (1978).
- [39] K. Nagel, *Phys. Rev. E* **53**, 4655 (1996); K. Nagel and M. Schreckenberg, *J. Phys. I* **2**, 2221 (1992); K. Nagel, in *Physics Computing '92*, edited by R. A. de Groot and J. Nadrchal (World Scientific, Singapore, 1993) p. 419; K. Nagel, Ph.D. thesis, University of Cologne, 1995.
- [40] H. C. Fogedby, *Phys. Rev. E* **68**, 026132 (2003).
- [41] A. Zoia, A. Rosso, and M. Kardar, *Phys. Rev. E* **76**, 021116 (2007).